

Research Article

Integrated Model Development for Tight Oil Sands Reservoir with 2D Fracture Geometry and Reviewed Sensitivity Analysis of Hydraulic Fracturing

¹Nguyen Huu Truong, ²Wisup Bae and ¹Hoang Thinh Nhan

¹PetroVietnam University (PVU), Vietnam

²Sejong University, Seoul, South Korea

Abstract: In this study, oil production rate in tight oil reservoir is much declined due to low permeability reservoir of 0.5 mD, low porosity of 0.15%, high reservoir depth range from 9,962.5 ft to 10,037.5 ft, high closure pressure up to 4,842.59 psi among fractures that lead to poor fracture conductivity in the fractures of the reservoir. Usually, high closure pressure is easy to reduce conductivity very fast during oil production. Need to stimulate the reservoir in order to enhance oil production is important to successful project by the application of integrating model development for tight oil reservoir based on the two dimensional Perkins and Kern Nordgren Carter fracture geometry in term of the power law parameters of hydraulic fracturing by systematic of model as Normal faulting stress regime, fracturing fluid model, fracture geometry model, pressure model, material balance, proppant selection, fracture conductivity that have been presented in detail of the research. By series calculation and laboratory experimental for fracture conductivity under closure pressure and proppant fracture concentration of 1.5 lb/ft² that fracture conductivity of 5,700 mD.ft of Carbo-Lite ceramics proppant size of 20/40, proppant density of 169 lb/ft³. In order to estimate the effects of the operating fracturing parameters condition of hydraulic fracturing as the injection rate, injection time, leak-off coefficient on the fracture half-length, fluid efficiency, the net fracture pressure, productivity, dimensionless fracture conductivity, the sensitivity analysis has been proposed for the analysis. The research is provided the new tool for hydraulic fracturing stimulation in order to advance in knowledge for engineer in the field. The post fracture production has been shown about 7.4 fold of oil production increment.

Keywords: 2D PKN-C model, integrating model development, sensitivity analysis

INTRODUCTION

Hydraulic fracturing stimulation is a stimulation technique with the goal for enhancing well productivity that technique has widely been used in the petroleum industry today. The first fracturing treatment specially designed to simulate for well production was conducted in the Hugoton gas field, July 1947, on Kelpper well located in Grant County, KS. Because of equipment limitations, the zone was selectively fractured for stimulation and the pump power limitations fractured for the reservoir with high depth, high closure pressure. In the 1950s and the middle 1960s, the hydraulic fracturing stimulation was developed with the high pump power to pump with high injection rate for the reservoir with high depth and high closure fracture pressure. At that time, the hydraulic fracturing fluid was continually developed to pump with high fluid efficiency. The technology has been continuously developed for well stimulation by hydraulic fracturing has become the best tool in the petroleum industry

today. In this study the tight oil sands reservoir with low permeability range of 0.1 md to 0.5 md and reservoir porosity range from 10 to 15 % and low effective wellbore radius of oil production has been declined, high heterogeneity geological structural lead to poor fracture conductivity among the fractures. The challenging to deal with the problem to simulate the oil reservoir by an integrated model development of hydraulic fracturing with two dimensional Perkins and Kern Nordgren Carter (2D PKN-C) fracture geometry for the tight oil reservoir for enhancing oil production are important part of the success project. For an integrated model development consists of these procedures are of the reservoir properties, selection the type of fracturing fluid in term of power law parameters, proppant selection under closure pressure of 4,842.59 psi, the fracture geometry model with spurt loss and leak-off coefficient, pressure model, material balance, effective wellbore radius and dimensionless fracture conductivity have been discussed.

Corresponding Author: Wisup Bae, Sejong University, Seoul, South Korea

This work is licensed under a Creative Commons Attribution 4.0 International License (URL: <http://creativecommons.org/licenses/by/4.0/>).

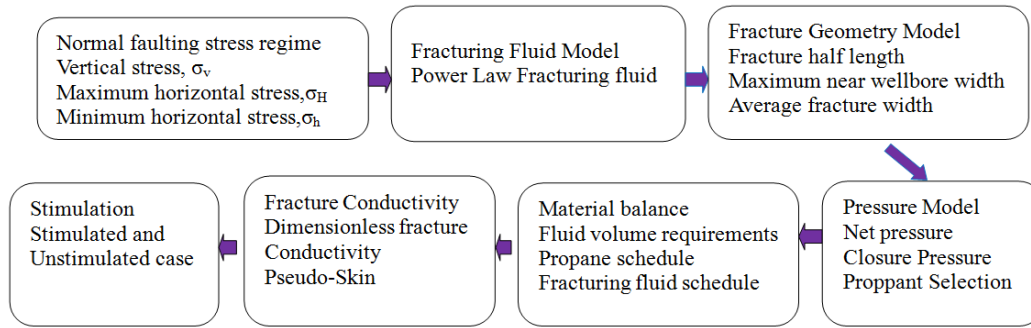


Fig. 1: Integrated model development of hydraulic fracturing for tight oil reservoir

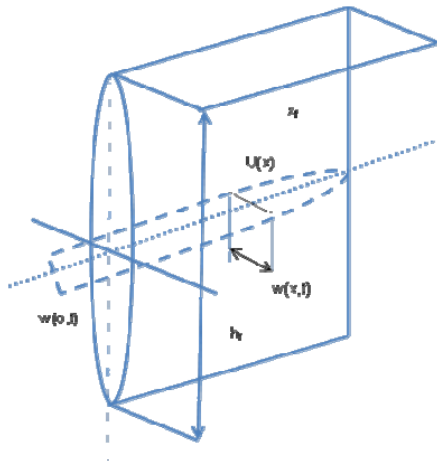


Fig. 2: Proppant concentration schedule

MATERIALS AND METHODS

Integrated model development and application: To calculate the values of the parametric fracture treatment parameters, then the integrated model development of hydraulic fracturing for sandstone reservoir with 2D fracture geometry are required in the field with several procedures are shown in the Fig. 1, the new model proposed here and discussed.

Normal faulting stress regime: During proppant slurry is pumped into the well with high pressure for producing fracture width and fracture propagation are along the fractures of the normal to the smallest of the principal stress, which can be saved the fracturing cost with minimum in-situ stress and low cost of pumping horsepower. Consequently the net fracture pressure at the near wellbore is maximized to provide more fracture growth and give the better fracture conductivity to increase the production ratio. Moreover, in a normal faulting stress regime with the vertical stress is maximized value one and the rest of the maximum horizontal stress, minimum horizontal stress are less than vertical stress.

Fracturing fluid model: In order to evaluate these fracture dimensions as the fracture length, maximum

width, average width, net pressure at the near wellbore, fluid efficiency. Hence, the power law parameters is precisely formed these parametric treatment design.

In hydraulic fracture design, the fracturing fluids widely have been used of the power law model to describing the rheological behavior that is given by:

$$\tau = K\gamma^n \quad (1)$$

where,

τ = Shear stress

γ = Shear rate

K = Consistency coefficient

n = Rheological index, (Valko and Economides, 1995).

The power law model can be expressed by:

$$\log \tau = \log K + n \log \gamma$$

Slope =

$$\frac{[(N \sum XY) - (\sum X \sum Y)]}{[(N \sum X^2) - (\sum X)^2]}$$

$$\text{Intercept} = (\sum Y - n \sum X) / N$$

where,

X = $\log \gamma$,

Y = $\log \tau$

N = Data number

Thus,

n = Slope

K = Exp (intercept)

Fracture geometry model: In this study a 2D Perkins-Kern-Nordgren (PKN; Perkins and Kern, 1961; Nordgren, 1972) model have been used to investigate the fracture propagations (Fig. 2). On other hand, the incorporations of Carter II solution (Howard and Fast, 1957), where the model has been presented as the 2D PKN-C fracture geometry account for the leak-off coefficient and spurt loss in term of power law parameters. In order to investigate exactly the fracture half-length and near wellbore fracture width forward the non-Newtonian fracturing fluid has been applied to form the results here, the maximal fracture width in the 2D PKN-C was presented in term of power law parameters as:

$$W_{w,o} = 9.15 \frac{1}{2n+2} \times 3.98 \frac{n}{2n+2} \left(\frac{1 + (\pi - 1)n}{n} \right)^{\frac{n}{2n+2}} \frac{1}{K^{2n+2}} \left(\frac{(q_i/2)^n h_f^{1-n} x_f}{E'} \right)^{\frac{1}{2n+2}} \quad (2)$$

where,

$$E' = \frac{1}{1-\nu^2}$$

where,

n = The power law behavior (dimensionless).

K = The consistency index (Pa-secⁿ).

ν = The Poisson's ratio.

The power law parameters are correlated with fluid viscosity of fracturing fluid (Rahman, 2008):

$$n = 0.1756(\mu)^{-0.1233}$$

$$K = 47.88 \times (0.5\mu - 0.0159)$$

The elliptical geometry the 2D PKN-C model is expressed of the average fracture width by introducing a shape factor of $\frac{\pi}{5}$, frequently the average fracture width (\bar{w}) along the fracture length was given by $W_{w,o} \frac{\pi}{5}$. By using Carter equation II with average fracture width, the expression of fracture half-length is performed as equation below:

$$x_f = \frac{(2S_p + \bar{w}) q_i}{4\pi C_L^2 h_f} \left[\exp(\beta^2) \operatorname{erfc}(\beta) + \frac{2\beta}{\sqrt{\pi}} - 1 \right] \quad (3)$$

where,

$$\beta = \frac{2C_L \sqrt{\pi t}}{w + 2S_p}$$

$$P_{net} = \frac{E'}{2h_f} W_{w,o} \quad (4)$$

In Eq. (3) has been presented the fracture half-length during fracture propagation account for the overall fluid leak-off and spurt loss with injection time. From the close of these equations is either fracture half-length or injection time can be easily determined using a numerical root-finding method. To calculate the fracture height, the fracture half-length, injection time and injection rate are known lead to calculate its fracture height by solving in the Eq. (3) by using an iterative method when power law fracturing fluid applied here. In addition to the power law parameters of n, K, pump rate (q_i), fracture height, Plain strain modulus (E'), the overall leak-off coefficient and spurt loss, are also known from these Eq. (1) to Eq. (3), which can be calculated the fracture half-length by using an iterative method.

The net fracture pressure of the fracture is a very important part to propagate fractures and produce

fracture width, which is used for predicting the fracture growth as well fracture half length, near wellbore fracture width and in the rest of the parameters are the closure stress, friction pressure lost along the tubing, injection rate are usually affected to pump horsepower and net fracture pressure.

Pressure model: During fracturing slurry is pumped down the well for cracking fractures and fracture propagation under the magnitude of the net pressure in the fractures, in which the net pressure is the total of surface treating pressure plus with wellbore fluid pressure minus the total of the friction losses inside tubing, perforation, tortuosity and closure pressure. Thereafter, the fractures will be propagated when the bottom hole pressure overcomes the closure pressure of fractures or exceeding the closure pressure, this stresses starts acting on the rock exceed the compressive or tensile failure of the rock. These stresses are relative with pump horse power and selective pump power requirement for injecting fracturing, if the fracture was high closure pressure and the proppant transport with the high friction losses occasionally need to select the high pumping power. In the fracturing operation, the following models were expressed in brief for net pressure and pumping horse power is given by:

$$P_{net} = P_{inj} + P_{head} - P_{tubing\ friction} - \Delta P_{pf} - \Delta P_{tort} - P_c \quad (5)$$

$$HHP = \frac{(P_{tubing\ friction} + \Delta P_{pf} + \Delta P_{tort} + P_c - P_{head})}{40.8} \quad (6)$$

where,

- P_{net} = The net pressure in fractures in psi
- P_{inj} = The injection pressure as surface treating pressure in psi
- P_{head} = The wellbore fluid pressure due to its depth and its slurry concentration in psi
- P_{tubing friction} = The tubing friction pressure lost due to the fracturing fluid effect on wellbore in psi
- ΔP_{pf} = The pressure loss through the perforation in psi
- ΔP_{tort} = The pressure loss due to tortuosity pressure effect in psi
- P_c = The closure pressure in psi and HHP is the horse power of injection

Material balance: In fracturing operation, during slurry pumping into the well for fractures growth and propagation, then the magnitude of fracture dimensions are as well as the fracture volume increase in pumping time that depends on the amount of the fluid volume lost in the fracture area and the fluid volume of spurt lost. Oftentimes if high fluid volume lost into the fracture area leads to decrease the fracture volume and fluid efficiency. Generally, the material balance was described here:

$$V_i = V_f + V_l$$

Table 1: Proppant data

Parameter	Value
Proppant type	20/40 CARBO-Lite
Specific Gravity	2.71
Strength	Intermediate
Diameter	0.0287 in
Packed porosity	0.35
Conductivity at 4,842.59 psi closure pressure (at 1.5 lb/ft ²)	5,700 md-ft.
Conductivity damage factor	0.5

where,

V_i = The total fracturing fluid volume pumped

V_f = The fracture volume

V_l = The total fluid loss volume in the fracture area

For the fracture volume, V_f , is expressed of a two wing of symmetrical fracture of $V_f = 2h_f x_f \bar{w}$. Additionally with the efficient fluid is presented as the ratio of fracture volume divided by the total volume pumped of V_f/V_i . Nolte (1986), have proposed for a relative approximation between the total volumes pumped down the well with pad volume pumped and also introduced a model for proppant concentration schedule. In order to investigate the fluid efficiency for hydraulic fracturing, the pad volume pumped should be design in pre-fracture treatment because it is occasionally affected to fluid efficiency. With high pad volume pumped into the well demonstrated that fluid efficiency is a given lower.

Proppant selection: Proppant properties have been decided to the fracture conductivity and dimensionless fracture conductivity under closure pressure in the field to relate the proppant fracture concentration. In order to estimate the fracture conductivity the proppant properties are of proppant shape, proppant size, proppant density, proppant porosity to effect on fracture conductivity under effective stress in reservoir. Generally, the high closure pressure should be selected with the high strength proppant. In this study, closure pressure of the fracture in this research of 4,842.59 psi that is basically to select strength of proppant is much more than 4,842.59 psi. In this case, the intermediate strength proppant-CARBO-Lite ceramics of 20/40 was selected for project (Economides and Nolte, 2000). By combining the value proppant fracture concentration plots with their closure pressure that lead to calculate the valueable fracture conductivity, proppant permeability, proppant porosity under closure pressure in the real field (Table 1).

Fracture conductivity: The fracture conductivity are generally taken from laboratory test (API standard) based on the proppant type and realistic closure stress apply on its. The API standard test for proppant conductivity in the real data to measure linear flow through a proppant packed between steel plates under a certain pressure with proppant concentration test at 2 lb/ft². The most published data measured by according to the API test (Smith, 1997), which only apply at the

laboratory fracture capacity. Because of the fracture conductivity is a very important to calculate the dimensionless fracture conductivity whether is presented at experimental laboratory of API standard based on several input parameters as proppant type, proppant size, proppant shape, proppant porosity, proppant permeability, proppant concentration, typical fracturing fluid and closure stress. In the past decades, several authors have introduced to predict the fracture conductivity by the relationship between proppant fracture concentration with closure fracture pressure by Darin and Huitt. Generally, the higher closures stress is given the lower fracture conductivity in order to predict precisely the value of fracture conductivity, these data consist of proppant type, proppant fracture concentration and the value of closure pressure are known for the field at pre-treatment. The higher proppant fracture concentration carried out API standard with closure pressure exerted on it that is given high fracture conductivity.

Production model: Based on the constant bottom hole pressure situation the oil production from fractured well in transient flow regime can be calculated by (Economides *et al.*, 1994):

$$p_i - p_{wf} = \frac{162.6q_0B\mu}{kh} \left(\log t + \log \left(\frac{k}{\phi\mu c_t r_w^2} \right) + s_f - 3.23 \right) \quad (7)$$

In which,

r_w' = The effective wellbore radius as given by:
 $r_w' = r_w e_f^{-s}$.

s_f = Pseudo-skin is calculated by the relationship (Valko *et al.*, 1997):

$$s_f = F - \ln \left(\frac{x_f}{r_w} \right)$$

where,

x_f = The fracture half-length.

r_w = The wellbore radius.

The F factor can be calculated by:

$$F = \frac{1.65 - 0.328u + 0.116u^2}{1 + 0.18u + 0.064u^2 + 0.005u^3} \quad (8)$$

where, $u = \ln(F_{CD})$ and F_{CD} is the dimensionless fracture conductivity which is calculated by $F_{CD} = \frac{k_f w_p}{k x_f}$, also F_{CD} is related to proppant number which is along the penetration ratio ($I_x = 2x_f/x_e$) and $k_f w_p$ is the fracture conductivity which can be calculated by experimental laboratory or fracture conductivity simulation when knowing a proppant fracture concentration in lb/ft² inside fracture under closure pressure to account on the proppant laden. Basically, the proppant number is defined by (Economides and Martin, 2007):

Table 2: Reservoir parameters

Parameter	Value
Target fracturing depth, ft.	10,000
Reservoir drainage area, acres	200
Reservoir drainage radius, ft.	1.667.25
Wellbore radius, ft.	0.328
Reservoir height, ft.	75
Reservoir porosity	0.15
Reservoir permeability, md	0.5
Reservoir fluid viscosity, cp	1.5
Oil formation volume factor, RB/STB	1.1
Total compressibility, psi ⁻¹	1.00 × 10 ⁻⁵
Initial reservoir pressure, psi	5,500
Flowing bottom hole pressure, psi	3,500
Closure pressure, psi	4,842.59

Table 3: Fracturing parameters

Parameter	Value
Fracture height, h _f , ft.	70.0
Sandstone Poisson's ratio	0.25
Leak-off coefficient, ft/min ^{0.5}	3.00 × 10 ⁻³
Young's modulus, psi	3.00 × 10 ⁶
Injection rate, bpm	40.0
Injection time, min	90.0
Spurt loss, in	0.00
Proppant concentration end of job, ppg	8.00
Flow behavior index, n	0.55
Consistency index, K, lbf.s ⁿ /ft ²	0.04
Fracturing fluid type: Borate-Crosslinked 30 lb HPG/1,000 gal with 8 lb/1,000 gal persulfate breaker additive	
Proppant type: (ISP) CARBO-Lite Ceramics 20/40, 169 lb/ft ³	

$$N_{propp} = \left(\frac{2k_f}{k_{res}} \right) \times \frac{V_{prop}}{V_{res}} \quad (9)$$

where,

k_f = The effective proppant pack permeability in mD

k = The reservoir permeability in mD

V_{prop} = The propped volume in the pay zone (two wings, including void space between the proppant grains) in ft³

V_{res} = The drainage volume in ft³

In the transient production period is often short time oil production (Table 2).

Application to a sandstone reservoir: By application an integrated model development for hydraulic fracturing has been presented for a typical sandstone reservoir having reservoir permeable layer. This is just taken from different sources (Economides *et al.*, 1994) and Rahman *et al.* (2003) for investigating the treatment parameters. The sandstone layer has underlying and overlying shale layer is fractured with single stage, which is as follow: 9,962.5-10,037.5 ft (Table 3).

RESULTS AND DISCUSSION

Proppant schedule: Figure 2 shows the proppant concentration schedule during proppant slurry is pumped to the well and the figure has been presented of how proppant is added into fracturing fluid for rising proppant concentration during injection with time until proppant concentration end of the job (8ppg). This is, however, not practical for the reason that beyond the point where the hydraulic width is smaller than three proppant diameters, the hydraulic fracture can no longer accept any proppant (Valko and Economides, 1995) by Rahman and Rahman (2010). A deeper layer having a higher fracture length needs more pad volume and pad time before proppant loading starts, which is very consistent. In the pad volume injected stage is about 57 min of injection rate of 40 bpm with 95,716 gallons and given the proppant slurry injected stage is about 33 min of injection rate of 40 bpm, the post fracture shows the fluid efficiency of 22.4%. Figure 2 is very consistent (Table 4).

In the transient production analysis as presented in the Fig. 3, the oil production in the both unstimulated case and stimulated case are in short time for oil production rate with time of 400 days. The figure also shows to us the oil production in the stimulated case is much more oil production compare to the oil production in the unstimulated case (Table 5).

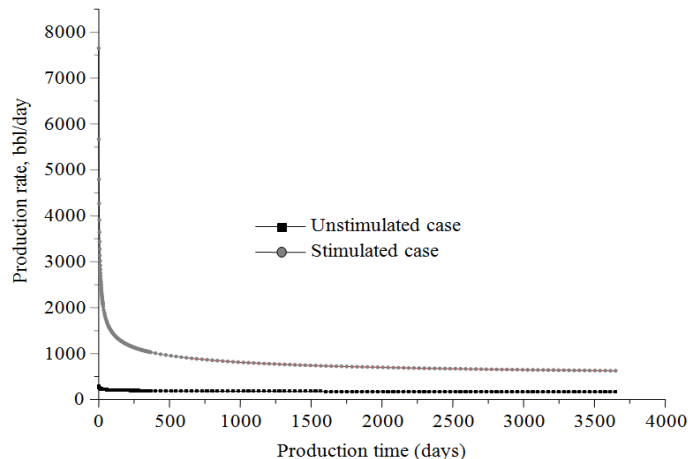


Fig. 3: Transient flow of unstimulated case and stimulated case

Table 4: Results from material balance

Parameter	Value
Fracture half-length, ft.	1,287.69
Max. Width, w_{wo} , in	0.45
Average width, \bar{w} , in	0.28
Total volume injected, gallons	151,200
Fracture volume, gallons	31,709
Fracture Area, ft ²	180,277
Fluid efficiency, %	22.4
Net Fracture pressure, psi	904
Proppant fracture concentration, lb/ft ²	1.5
Average proppant concentration, ppg	4.9
Pad volume pump, gallons	95,716
Time to pump pad volume, min	57
Total fluid volume loss, gallons	119,491
Mass of proppant, lb.	271,808

Table 5: Simulation to CARBO-Lite ceramics 20/40, 169 lb/ft³ plots with closure pressure of 4,842.59 psi and fracture concentration and production analysis

Parameter	Value
Closure pressure, psi	4,842.59
Fracture conductivity, mD-ft	5,700
Dimensionless fracture conductivity, F_{CD}	4.4
Pseudo-skin	-7.4
Effective wellbore radius, ft	523
Fold increase	7.4

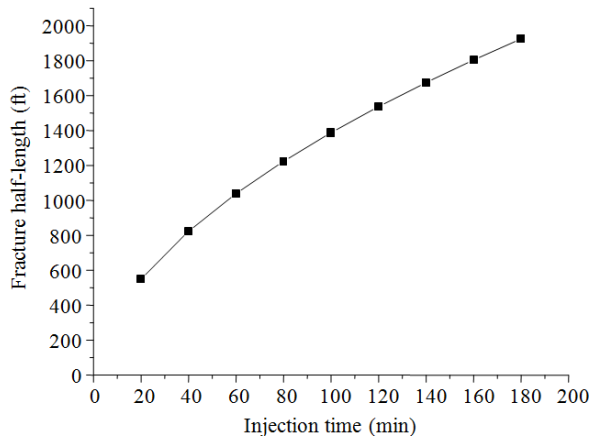


Fig. 4: The effect of the injection time on the fracture half-length

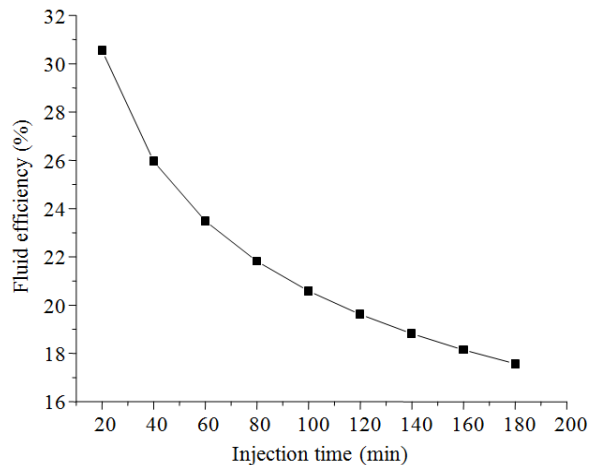


Fig. 5: The effect of the injection time on the fluid efficiency

Sensitivity analysis: In order to understand how changes in parameters affect to the fracture half-length, fracture conductivity, productivity ratio and fluid efficiency of the fractured well, the sensitivity analysis has been conducted for this purpose of the research. In this study the 2D PKN-C fracture geometry model has been selected to perform the effects of the parameters are of injection rate, leak-off coefficient and injection time to fracture half-length of course productivity ratio in post-fracture. The model is chosen in terms of the standard model. Sensitivity analysis only one parameter of the model has been changed and the rest of the parameters keeping with the standard design system.

The effect of injection time on the fracture half-length: Figure 4 shows the injection time versus fracture half-length, the figure also presented when only an increase in the injection time at various times of 20, 40, 60 min, respectively etc., lead to increase the fracture half-length because this reason can be explained with increase in the injection time as well increasing slurry volume requirement injected into the well, which is directly proportional to the fracture half-length of course more slurry volume with time is given more fracture half-length in the limited fluid leak-off into fracture surface area based on the material balance in the 2D PKN-C fracture geometry model with the remains the constant fracture height at the near wellbore.

The effect of the injection time on the fluid efficiency: Figure 5 shows to us the injection time versus the fluid efficiency; the figure is also presented that the increasing injection time leads to decrease the fluid efficiency due to the more injection time is more fracture half-length of course given more fracture width leads to increase the fracture surface area of the fracture. Moreover, to account for fluid volume lost into the surface area of the fractures with time during fracturing, which is directly proportional to the total fracture surface area of course more surface fracture area is a more fluid volume loss. Based on the material balance of the 2D PKN-C fracture geometry model shows in the more fluid volume loss is less fracture volume as low fluid efficiency as presented in Fig. 3.

The effect of the injection time on the net fracture pressure: Figure 6 is presented the net fracture pressure versus the injection time based on the 2D PKN-C fracture geometry with keeping the fracture height constant of 70 ft at the near wellbore and remains the constant injection rate of 40 bpm with increasing injection time and only changing injection times during fracturing. The figure is also depicted that with increasing injection time as 20, 40 min, etc., lead to increase the net fracture pressure. This is because when the increase in injection time as well increases in the

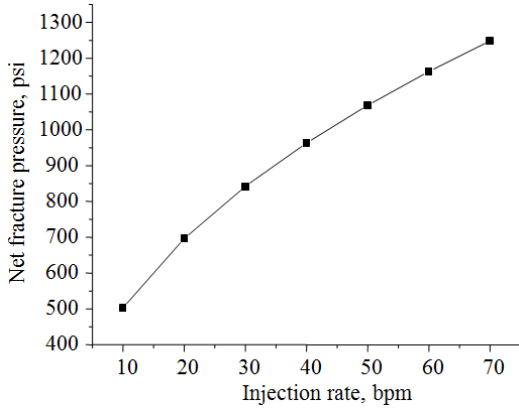


Fig. 6: The effect of the injection time on the net fracture pressure

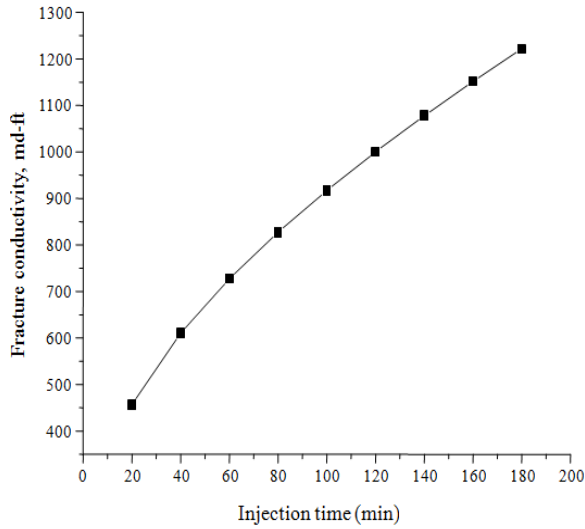


Fig. 7: The effect of the injection time on fracture conductivity

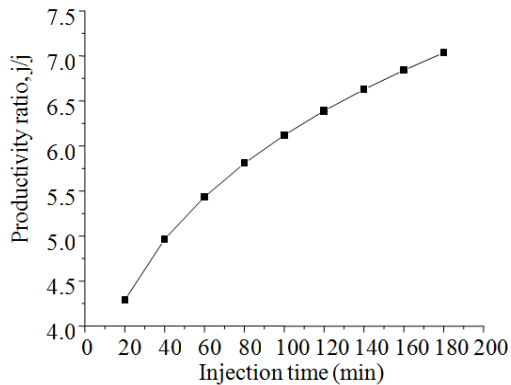


Fig. 8: The effect of injection time on the productivity ratio

fracture half-length due to increasing injection volume as presented in Fig. 4 to increase the fracture width, which is directly proportional to the net fracture pressure for more fracture width is given more net fracture pressure as performed in Fig. 4.

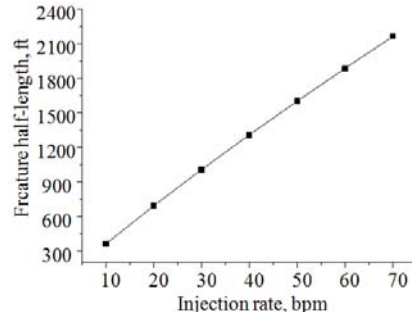


Fig. 9: The effect of the injection rate on the fracture half-length

The effect of the injection time on fracture conductivity: Figure 7 shows to us the injection time versus fracture conductivity; the figure also is presented the increasing injection time at differential times of 20, 40, 60 min, respectively etc., lead to increase the fracture conductivity. This is because that the longer injection time as large injection volume into the well is given more fracture growth along fracture half-length. Based on the 2D PKN-C fracture geometry model with remains the constant injection rate of 40 bpm ordered to keeping the constant fracture height at the near wellbore. Consequently, the results in increasing fracture conductivity with longer injection time are very consistent as presented in Fig. 5.

The effect of the injection time on productivity ratio: Figure 8 is presented the injection time versus productivity ratio. The figure also shows in the increase injection time lead to increase in the productivity ratio. This is because the longer injection time is more injected volume into the well based on the constant injection rate of 40 bpm and give the longer fracture half-length is less pseudo-skin because the injected volume is directly proportional to fracture half-length. Consequently the productivity ratio is increased by increasing the injection time (Valko *et al.*, 1997).

The effect of the injection rate on the fracture half-length: Figure 9 is shown to us the effect of injection rate on the fracture half-length, the figure also is presented with the injection rate increase of 10, 20, 30, 40, 50 bpm, respectively etc., consequently fracture half-length increase. This is easily explained by Eq. 3, the injection rate is directly proportional to fracture half-length and based on the 2D PKN-C fracture geometry with the constant fracture height of 70 ft at the near wellbore.

The effect of the leak-off coefficient: The model for overall leak-off coefficient was presented by (Williams, 1970; Williams *et al.*, 1979) as:

$$C_l = \frac{-\frac{1}{c_c} + \sqrt{\frac{1}{c_c^2} + 4\left(\frac{1}{c_b^2} + \frac{1}{c_w^2}\right)}}{2\left(\frac{1}{c_b^2} + \frac{1}{c_w^2}\right)} \quad (10)$$

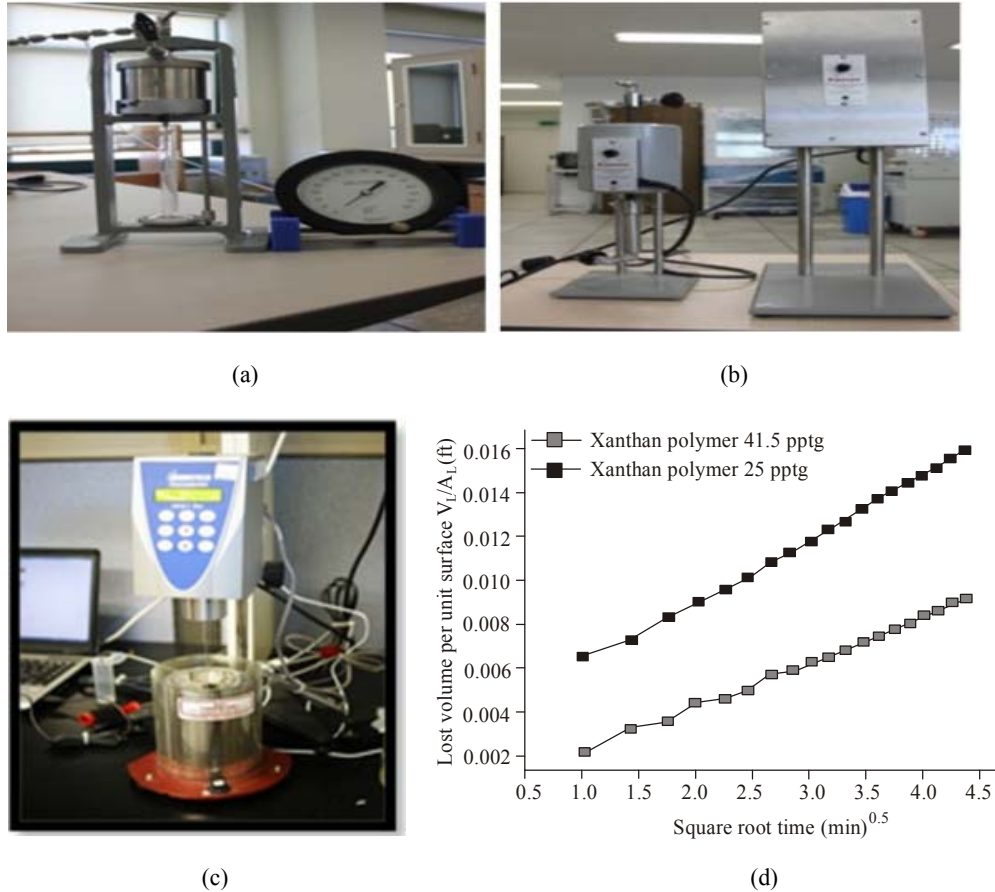


Fig. 10: Laboratory experiment at which; (a): Low-pressure Low-temperature (LPLT) filtration test; (b): High Pressure High Temperature (HPHT) filtration test and; (c): Measure the filtration viscosity; (d): The effects of the polymer concentration on wall building of fluid loss coefficient (C_w)

Formula is modified as:

$$\frac{2}{c_l} = \frac{1}{c_c} + \sqrt{\frac{1}{c_c^2} + 4\left(\frac{1}{c_v^2} + \frac{1}{c_w^2}\right)} \quad (11)$$

C_c = The compressibility fluid loss leak-off in reservoir conditions in $\text{ft}/\text{min}^{0.5}$

C_v = The viscous fluid loss coefficient in $\text{ft}/\text{min}^{0.5}$

C_w = The wall building of fluid loss coefficient in $\text{ft}/\text{min}^{0.5}$

The leak-off coefficient as overall fluid loss Coefficient (C_l) has been seen to become more important in treatment design parameters that affect to fracture geometry. The combining leak-off coefficient presented by the controlling three mechanisms as the compression of the reservoir fluids, the thickness of the invaded zone which is filled with the viscous fracture fluid and filter cake which presents as wall building effect coefficient that depend on the fluid additives, type of fluid, polymer concentration as presented in Fig. 10 and the condition of the reservoir as well temperature, pressure. In this study, 30 pound per

thousand gallons (pptg) of HPG polymer with 8 pptg of $\text{Na}_2\text{S}_8\text{O}_2$ breaker is given the leak-off coefficient of $0.003 \text{ ft}/\text{min}^{0.5}$, so the higher polymer concentration is lower wall building coefficient as lower overall leak-off coefficient due to the wall-building coefficient, compressibility fluid loss, viscous fluid loss in the reservoir conditions is directly proportional to the overall leak-off coefficient as presented in equation 8 and the lower polymer concentration is higher wall building coefficient for higher overall leak-off coefficient. On the effect of the leak-off coefficient on the fracture geometry as fracture half-length, fracture width and the net fracture pressure, conductivity, productivity ratio have been presented and discussed here based on the 2D PKN-C fracture geometry model.

Figure 11 presented the effect of leak-off coefficient on the fracture half-length, the higher leak-off coefficient is shorter fracture half-length due to it is inversely proportional to fracture half-length as presented in equation 3. Figure 12 is presented the leak-off coefficient with fluid efficiency, the figure shows when increasing the leak-off coefficient leads to decreasing fluid efficiency at the standard the PKN-C

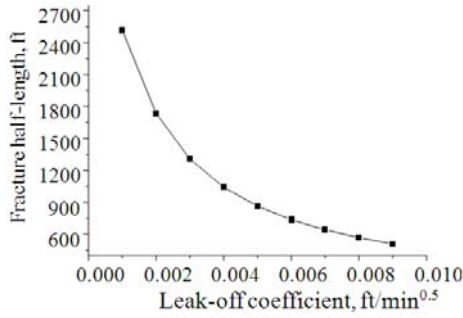


Fig. 11: The effect of leak-off coefficient on the fracture half-length

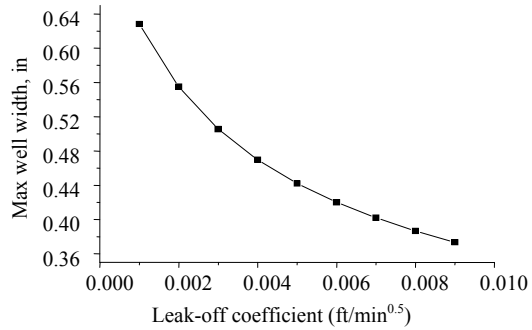


Fig. 14: The effect of the leak-off coefficient on the fracture width

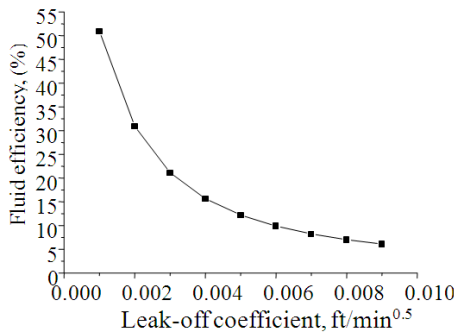


Fig. 12: The effect of the leak-off coefficient on the fluid efficiency

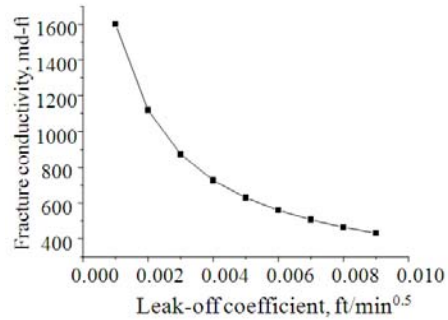


Fig. 15: The effect of the leak-off coefficient on fracture conductivity

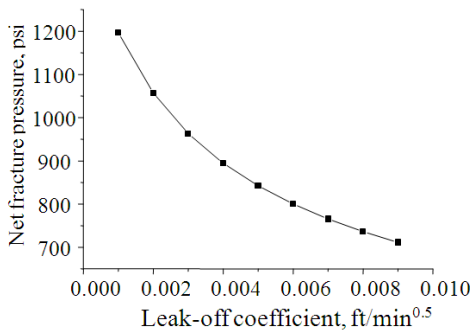


Fig. 13: The effect of the leak-off coefficient on the net fracture pressure

fracture geometry and constant fracture height of 70 ft with increasing in the leak-off coefficient. This is because the increasing leak-off coefficient as decreasing fracture volume due to total injected volume into the well constant with injection time is equal to fracture volume plus with volume fluid loss, the high leak-off coefficient is more fluid volume loss as decreasing fracture volume leads to decreasing fluid efficiency. Moreover, with the more fluid volume loss at high leak-off coefficient as 0.004, 0.005, 0.006, 0.007 ft/min^{0.5}, respectively as less polymer concentration compare to the leak-off coefficient of 0.003 ft/min^{0.5}, which are shorter fracture half-length and narrow fracture width as less fracture volume. In the field the leak-off coefficient depends on several

parameters as the polymer concentration, fluid additive, reservoir properties. On the other hand, only fracturing fluid can be controlled by designing the fracturing fluid viscosity in polymer concentration, also fluid additives and the rest of the other parameters are reservoir permeability, porosity, fluid flow viscosity, reservoir temperature, reservoir pressure, oil saturation, water saturation, rock compression are uncontrolled but their most affected to the overall leak-off coefficient.

Figure 13 is shown the leak-off coefficient versus net fracture pressure, the high leak-off coefficients as 0.004, 0.005, 0.006, 0.007, respectively compare to the leak-off coefficient of 0.003 ft/min^{0.5}, which are decreased the net fracture pressure. Moreover, the high leak-off coefficient is the reduced net fracture pressure due to more leak-off coefficient is shorter fracture half-length and narrow fracture width, which fracture width is directly proportional to net fracture pressure based on the PKN-C fracture geometry keeps the standard design and constant fracture height.

Figure 14 is performed the leak-off coefficient versus fracture width, the figure also is shown that the high leak-off coefficient is the narrower fracture width and the low leak-off coefficient is wider fracture width. This is due to the high leak-off coefficient of 0.004, 0.005, 0.006, 0.007 ft/min^{0.5}, respectively are the shorter fracture half-length compare to the fracture half-length in the leak-off coefficient of 0.003 ft/min^{0.5}. The material balance has been shown that the leak-off coefficient is inversely proportional to the fracture half-

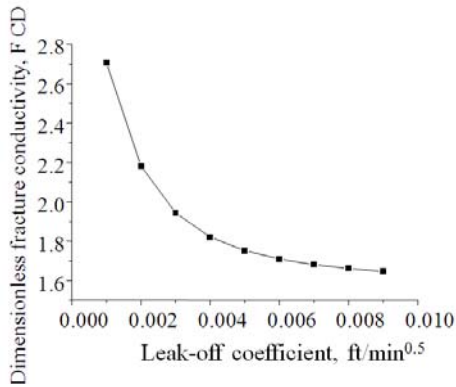


Fig. 16: The effect of the leak-off coefficient on the dimensionless fracture conductivity

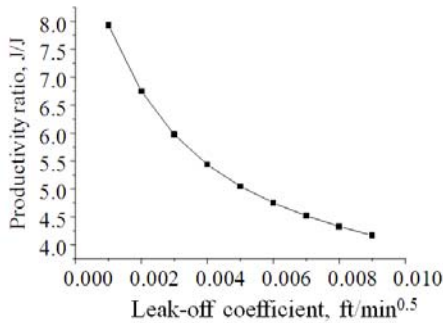


Fig. 17: The effect of the leak-off coefficient on the productivity ratio

length, the high leak-off coefficient is shorter fracture half-length as narrow fracture width due to the fracture width is directly proportional to fracture half-length.

Figure 15 is presented the leak-off coefficient versus the fracture conductivity; the figure also depicted that the high leak-off coefficient as lower polymer concentration in fracturing fluid as explained in equation 8, the lower polymer concentration is higher wall building coefficient fluid loss. One other hand, the C_w is directly proportional to the overall leak-off coefficient, which is the lower fracture conductivity. This is because the high leak-off coefficient as 0.004, 0.005, 0.006 ft/min^{0.5}, respectively compared to 0.003 ft/min^{0.5} in 30 pounds per thousand gallons (pptg), which are the narrower fracture width of course the shorter fracture half-length.

Figure 16 is presented the leak-off coefficient versus dimensionless fracture conductivity and Fig. 17 is presented the leak-off coefficient versus productivity ratio. Figure 16 shows when the leak-off coefficient is increased of 0.004, 0.005, 0.006 ft/min^{0.5}, respectively as decreasing the polymer concentration of fracturing fluid, which are less than 30 pounds per thousand gallons (pptg), the higher leak-off coefficients decrease the dimensionless fracture conductivity. To optimum dimensionless fracture conductivity is about 1.6 (Valko

et al., 1997) and the optimum dimensionless fracture conductivity is of 1.3-1.6 (Richardson, 2000). This is because the high leak-off coefficient is the shorter fracture half-length of course the narrower fracture width due to fracture half-length is directly proportional to the fracture width. Moreover, fracture width is directly proportional to dimensionless fracture conductivity as present in Eq. (12). Consequently, the narrow fracture width is less dimensionless fracture conductivity whereas the wider fracture width is larger dimensionless fracture conductivity.

The dimensionless fracture conductivity, F_{CD} can be identified as (Cinco-Ley et al., 1978):

$$F_{CD} = \frac{k_{wf}}{k \times x_f} \quad (12)$$

where,

k_{wf} = The fracture conductivity (md-ft)

k = The reservoir permeability (md)

x_f = The fracture length in ft

CONCLUSION

In this study, the application of the integrated model development for hydraulic fracturing stimulation to tight oil reservoir with the 2D PKN-C fracture geometry and from the sensitivity analysis may be summarized as follows:

- The sensitivity analysis is best tool to estimate the effects of operating fracturing parameters as injection rate, injection time; leak-off coefficient have been presented as Fig. 10 until 17.
- The 2D PKN-C is the best fracture geometry to stimulate the tight oil reservoir account for the spurt loss, leak-off coefficient in the field in term of power the law parameters as consistency index (K) and flow behavior index (n) to get the fracture half-length and fracture width of hydraulic fracturing stimulation.
- In the post fracture production is shown about 7.5 of fold oil production increment this result of oil production is much higher than the unstimulated case.
- The best design leak-off coefficient in the pre-fracturing can be found the optimum dimensionless fracture conductivity of 1.6.

REFERENCES

Cinco-Ley, H., V.F. Samaniego and A.N. Dominguez, 1978. Transient pressure behaviour for a well with a finite conductivity vertical fracture. Soc. Petrol Eng. J., 18: 253-264.

- Economides, M. J. and Nolte, K. G. 2000. Reservoir Stimulation. Third Edn. New York: John Wiley & Sons.
- Economides, M.J., A.D. Hill and C.E. Ehlig-Economides, 1994. Petroleum Production Systems. Prentice Hall, Upper Saddle River, NJ.
- Economides, M.J. and T. Martin, 2007. Modern Fracturing: Enhancing Natural Gas Production. ET Publishing, United States of America.
- Howard, G.C. and C.R. Fast, 1957. Optimum fluid characteristics for fracture extension. Drilling and Production Prac., API, pp: 261-270, (Appendix by E.D. Carter).
- Nolte, K.G., 1986. Determination of proppant and fluid schedules from fracturing-pressure decline. SPE Prod. Eng., 1(04): 255-265.
- Nordgren, R.P., 1972. Propagation of a vertical hydraulic fracture. Soc. Petrol. Eng. J., 12(4): 306-314.
- Perkins, T.K. and L.R. Kern, 1961. Width of hydraulic fractures. J. Petrol. Technol., 13(9): 937-949.
- Rahman, M.M., M.K. Rahman and S.S. Rahman, 2003. Optimizing treatment parameters for enhanced hydrocarbon production by hydraulic fracturing. J. Can. Petrol. Technol. 42: 38-46.
- Rahman, M.M., 2008. Productivity prediction for fractured wells in tight sand gas reservoirs accounting for non-darcy effects. Proceeding of the SPE Russian Oil and Gas Technical Conference and Exhibition. Moscow, Russia, October 28-30.
- Rahman, M.M. and M.K. Rahman, 2010. A review of hydraulic fracture models a development of an improved pseudo-3D model for stimulating tight oil/gas sand. Energ. Source Part A, 32: 1416-1436.
- Smith, M.B., 1997. Hydraulic Fracturing. 2nd Edn., NSI Technologies, Tulsa, Oklahoma.
- Valko, P. and M.J. Economides, 1995. Hydraulic Fracture Mechanics. John Wiley and Sons, Chichester, England.
- Valko, P., R.E. Oligney and M.J. Economides, 1997. High permeability fracturing of gas wells. Gas TIPS (Fall), 3(3): 31-40.
- Williams, B.B., 1970. Fluid loss from hydraulically induced fractures. J. Petrol. Technol., 22(7): 883-888.
- Williams, B.B., J.L. Gidley and R.S. Schechter, 1979. Acidizing Fundamentals. SPE Monograph, Vol. 6, Society of Petroleum Engineers of AJME, Richardson, TX.